

*Topology* Vol. 25, No. 3, pp. 353–373, 1986.  
Printed in Great Britain.

0040-9383/86 \$3.00 + .00  
© 1986 Pergamon Press Ltd.

## SMOOTH CONCORDANCE OF TOPOLOGICALLY SLICE KNOTS

ROBERT E. GOMPF

(Received 28 January 1985)

### §0. INTRODUCTION

THE SET of smooth knots  $S^1 \subset S^3$  (up to isotopy) is of great interest to low-dimensional topologists. A standard method for studying this set is to turn it into a group, by means of an equivalence relation called *smooth concordance*. Roughly speaking, two knots  $K_0$  and  $K_1$  are smoothly concordant if there is a smoothly embedded annulus in  $S^3 \times I$  with boundary  $K_0 \times 0 \cup K_1 \times 1$ . The set  $\mathcal{K}_{\text{DIFF}}$  of smooth concordance classes of knots is an abelian group under the operation of band-connected sum (respecting string orientations). Elements of the identity class are called *smoothly slice*. A smoothly slice knot in  $S^3 = \partial B^4$  is one which bounds a smoothly embedded 2-disk in  $B^4$ .

The group  $\mathcal{K}_{\text{DIFF}}$  may be studied by forming several quotient groups. In particular, we obtain the *topological concordance group*  $\mathcal{K}_{\text{TOP}}$  by allowing flat topological annuli in the above discussion, rather than just smooth ones. Inclusion gives a canonical epimorphism  $i: \mathcal{K}_{\text{DIFF}} \rightarrow \mathcal{K}_{\text{TOP}}$  whose kernel is the group of smooth concordance classes of knots which are *topologically slice*, i.e., which bound flat topological disks in  $B^4$ . The group  $\mathcal{K}_{\text{TOP}}$  can be collapsed still further, by modding out the subgroup of *algebraically slice* knots to obtain a group  $\mathcal{K}_{\text{ALG}}$ . (Specifically, a knot is algebraically slice if it has a Seifert surface whose Seifert form vanishes on a half-dimensional subspace. This is an invariant of topological concordance.)

The group  $\mathcal{K}_{\text{ALG}}$  is well-understood. (It contains a free abelian group of infinite rank, as well as 2- and 4-torsion.) We would also like to understand the kernels of the maps  $\mathcal{K}_{\text{DIFF}} \rightarrow \mathcal{K}_{\text{TOP}} \rightarrow \mathcal{K}_{\text{ALG}}$ . In higher dimensions, the corresponding kernels vanish;  $\mathcal{K}_{\text{DIFF}} = \mathcal{K}_{\text{TOP}} = \mathcal{K}_{\text{ALG}}$ . In our situation, however, this is false. By means of Casson–Gordon invariants, it has been shown that the kernel of  $\mathcal{K}_{\text{TOP}} \rightarrow \mathcal{K}_{\text{ALG}}$  contains a free abelian group of infinite rank.

The remaining map  $i: \mathcal{K}_{\text{DIFF}} \rightarrow \mathcal{K}_{\text{TOP}}$  has resisted any analysis until quite recently, since all available tools have been basically topological. This situation has now changed, due to Donaldson’s Theorem [2].

Donaldson has proven that no smooth, closed, simply connected 4-manifold can have a nonstandard definite intersection form. The proof depends heavily on gauge theory, so the result is intrinsically smooth in nature. The theorem implies that in dimension 4, smooth surgery is impossible in many cases where topological surgery can be accomplished by Freedman theory. As a result, many locally flat topological embeddings of 2-spheres in 4-manifolds cannot be smoothed. This observation allows the construction of knots which are topologically slice, but not smoothly slice. (This was first noticed by Casson.) In the present paper, we use this theory to show that  $\ker i$  contains elements of infinite order.

We define a smooth concordance invariant, called *kinkiness*, which detects knots with infinite order in  $\mathcal{K}_{\text{DIFF}}$ . In §1 and §2 we exhibit a large collection of knots with infinite order in  $\ker i$ . While we do not actually prove that  $\ker i$  is larger than  $\mathbb{Z}$ , it now seems a good conjecture that  $\ker i$  contains a free abelian group of infinite rank. In §1, we construct (via an earlier paper [5]) knots with arbitrarily large kinkiness. Since kinkiness gives a lower bound

for the unknotting number, this also shows that there are Alexander polynomial one knots with arbitrarily high unknotting number. In §2, we use a different method to construct an explicit infinite family of “doubled” knots with nonzero kinkiness.

Doubling is a procedure for obtaining new knots from old ones. Freedman has shown that the double of any knot is topologically slice (since it has Alexander polynomial one). Since doubling is compatible with smooth concordance, it defines a function (of sets)  $D : \mathcal{K}_{\text{DIFF}} \rightarrow \ker i$ . The results of §1 imply that  $D$  is not onto (and not a homomorphism). In §2, we exhibit knots which may be doubled several times without becoming smoothly slice. In particular, the trefoil knot may be doubled up to 5 times (at least) and still have infinite order in  $\ker i$ . We also give an infinite family of twists knots which may be doubled up to 7 times and still have infinite order. It seems quite plausible that repeated doubling will never make these knots smoothly slice. (Note that these results depend crucially on the orientation conventions given in §2.)

### §1. KINKINESS OF KNOTS

For the remainder of this paper, we work in the smooth category unless otherwise stated.

Two knots  $K_0, K_1 : S^1 \rightarrow S^3$  are called *concordant* if there is an embedding of an annulus  $f : S^1 \times I \subset S^3 \times I$  such that for  $t = 0, 1$ ,  $f^{-1}(S^3 \times t) = S^1 \times t$ , and  $f|S^1 \times t$ , as a map from  $S^1$  to  $S^3$ , equals  $K_t$ . Note that the trivial annulus  $K_1 \times \text{id}$  shows that the inverse of  $K_1$  in  $\mathcal{K}_{\text{DIFF}}$  is given by  $K_1$  with reversed orientations on both  $S^1$  and  $S^3$  (i.e. the mirror image of  $K_1$  with reversed string orientation).

In [5], an invariant called “kinkiness” was defined for circles in boundaries of 4-manifolds. This was used to distinguish an infinite family of nondiffeomorphic Casson handles. We restate the definition for a knot  $K$  in  $S^3 = \partial B^4$ . Consider all self-transverse immersed disks in  $B^4$  with boundary  $K$ . Let  $k_+(K)$  be the minimum number of positive kinks (points of self-intersection) occurring in any such disk. Similarly, let  $k_-(K)$  be the minimum number of negative kinks in any such disk.

*Definition.* The *kinkiness* of the knot  $K$  is the ordered pair  $k(K) = (k_+, k_-)$  as defined above.

Thus, a smoothly slice knot has kinkiness  $(0, 0)$ . (Note that the converse is false; the figure-eight knot has kinkiness  $(0, 0)$  but is not slice.) Kinkiness is easily seen to be an invariant of smooth concordance; hence, it gives a map (of sets)  $k : \mathcal{K}_{\text{DIFF}} \rightarrow \mathbb{Z} \times \mathbb{Z}$ . Note that if we take the mirror image of a knot,  $k_+$  and  $k_-$  are interchanged, although  $k$  is independent of string orientation.

Let  $[K]$  denote the smooth concordance class of  $K$ .

**THEOREM 1.1.** *If  $k(K) = (0, n)$ ,  $n \neq 0$ , then  $[K]$  has infinite order in  $\mathcal{K}_{\text{DIFF}}$ .*

*Proof.* Suppose  $[K]$  has finite order  $r$ , i.e.,  $r[K] = 0$  ( $r \geq 2$ ). Then  $(r-1)[K] = -[K]$ . This is represented by the mirror image of  $K$ ; hence,  $(r-1)[K]$  has kinkiness  $(n, 0)$ . But  $k_+(K) = 0$ , so  $K$  bounds an immersed disk with no positive kinks. The same is clearly true for the connected sum of  $r-1$  copies of  $K$ , so  $k_+((r-1)[K]) = 0$ , not  $n$  as claimed above.

QED

Similar reasoning shows that if  $k(K) = (0, n)$ ,  $n \neq 0$ , then the connected sum of  $K$  with any knots having  $k_+ = 0$  will have infinite order. In §2, we will give an infinite collection of knots in  $\ker i$  (iterated doubles of twist knots) with kinkiness  $(0, 1)$ . In this section, we use the results of [5] to prove the following:

**THEOREM 1.2.** *For any integer  $n \geq 0$ , there is a knot  $K$  in  $\ker i$  with  $k(K) = (0, n)$ .*

*Proof.* Fix  $n > 0$ . In [5] we constructed a Casson handle  $CH_{0,n}$  whose first stage kinky handle has exactly  $n$  kinks, all negative.  $CH_{0,n}$  has the property that any immersed disk in  $CH_{0,n}$  spanning the attaching circle necessarily has at least  $n$  negative kinks. Furthermore, from the method of construction, it follows that this property is stable under connected sum with  $\mathbb{C}P^2$ 's; i.e., any spanning disk in  $CH_{0,n} \# (\#_m \mathbb{C}P^2)$  must have at least  $n$  negative kinks, provided that it is algebraically disjoint from the  $\mathbb{C}P^2$ 's.

Let  $T_6$  be the first 6 stages of  $CH_{0,n}$ . For each top stage core disk, blow up a  $\mathbb{C}P^2$  at each kink. We may then replace the core by an embedded disk. Note that at each negative kink, the new disk will run algebraically twice over the corresponding  $\mathbb{C}P^2$ , introducing 4 twists in the framing. (See [5] for a discussion of this.) Let  $T$  denote  $T_5$  union a tubular neighborhood of each new disk, inside  $T_6 \# (\#_m \mathbb{C}P^2)$ .  $T$  looks like a 6-stage tower with no kinks on the top stage, except that the top stage framings are wrong. In particular,  $T$  is diffeomorphic to  $B^4$ , but the attaching circle is some nontrivial knot  $K$  in  $\partial T$  (due to the twisted framings).

The knot  $K$  has kinkiness  $(0, n)$ . In fact,  $k_-(K) \geq n$  by previous remarks, since  $T$  is embedded in  $T_6 \# (\#_m \mathbb{C}P^2) \subset CH_{0,n} \# (\#_m \mathbb{C}P^2)$ . But  $K$  bounds the first stage core disk of  $T_5$  in  $T$ . This has no positive kinks and  $n$  negative kinks, so  $k(K) = (0, n)$ . Furthermore,  $T_5$  is a 5-stage tower, so it contains a flat topological disk spanning  $K$  [6]. Thus,  $K$  is in  $\ker i$ .

QED

Actually, it is sufficient to use the first 3 stages,  $T_3$ , in place of  $T_6$  in the above argument. Careful inspection shows that the resulting knot  $K$  will be a connected sum of  $n$  knots, each of which is a double of a connected sum of twist knots (i.e., the knots  $K_l$ ,  $l \geq 1$ , defined in §2). Since Freedman has shown that any double is topologically slice, it follows that  $K$  is in  $\ker i$ . (This also demonstrates that the doubling map  $D: \mathcal{K}_{\text{DIFF}} \rightarrow \ker i$  cannot be a homomorphism, for  $K$  is a connected sum of doubles, but it cannot be concordant to a double unless  $n = 0$  or 1.)

## §2. DOUBLES OF TWIST KNOTS

In this section, we show that many iterated doubles of twist knots have kinkiness  $k = (0, 1)$ . We do this modulo the main lemma, which is proven in §3. We also give other applications of the main lemma in this section.

Given a knot  $K$ , we define its double,  $DK$ , as follows: Consider the solid torus  $T$  with inscribed circle  $C$  shown in Fig. 1. Map  $T$  diffeomorphically to a tubular neighborhood of  $K$ , so that (1) the orientation of  $T$  is preserved, and (2) an untwisted longitude in  $\partial T$  goes to a pushoff of  $K$  defining the 0-framing. Define  $DK$  to be the image of  $C$  (well defined up to isotopy). Let  $D^n K$  be the knot obtained from  $K$  by  $n$  successive doublings.

Note that we require our doubles to be untwisted, and to have negative clasps as in Fig. 1.

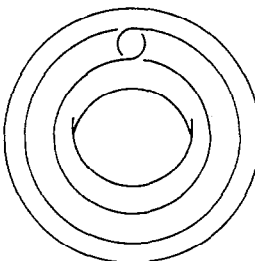


Fig. 1.

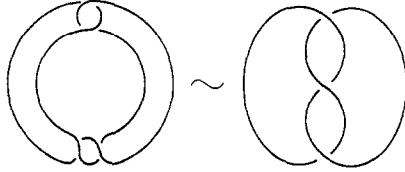


Fig. 2.

(If we consider the figure in  $S^3 = \partial B^4$ , then  $C$  clearly bounds an immersed disk in a small neighborhood of  $T$  in  $B^4$ . This disk has a single kink, which is negative.) It follows that the kinkiness of any double must be  $(0, 0)$  or  $(0, 1)$ .

We let  $K_l$  denote the “ $l$ -twisted double” of the unknot. That is, we form  $K_l$  from Fig. 1 by putting  $l$  right-handed twists in  $T$ . Thus,  $K_1$  is the left-handed trefoil knot shown in Fig. 2.

**THEOREM 2.1.** *The trefoil and its first 5 doubles ( $D^n K_1$ ,  $0 \leq n \leq 5$ ) have kinkiness  $k = (0, 1)$ . Similarly, for  $l > 1$ ,  $K_l$  and its first 7 doubles ( $D^n K_l$ ,  $0 \leq n \leq 7$ ) have  $k = (0, 1)$ .*

Thus, all of the above knots  $D^n K_l$  have infinite order in  $\mathcal{K}_{\text{DIFF}}$ . Furthermore, those with  $n \geq 1$  all lie in  $\ker i$  by Freedman’s results. Note that orientations are crucial here, since  $K_{-2}$  is the Stevadore’s knot, which is smoothly slice. Theorem 2.1 follows from Lemma 2.3, which we will state after developing suitable notation.

Let  $T_n$  denote the  $n$ -stage tower with a single kink at each stage, and all kinks negative. (For the theory of towers, see [3] or [6].) Construct  $\tilde{T}_n$  from  $T_n$  and a 4-ball  $B^4$  by gluing  $T_n$  onto an unknot in  $\partial B^4$  with framing  $-1$ . Now construct  $\tilde{T}_{n,l}$  from  $\tilde{T}_n$ , as follows: Find a standard framed circle on the top stage of  $T_n$ , such that attaching a kinky handle along this would yield  $T_{n+1}$ . Now add a 2-handle to this curve on  $\tilde{T}_n$ , with  $l$  right twists relative to the standard framing. Thus,  $\tilde{T}_{n,0}$  is a  $-1$  Hopf bundle, since the tower collapses to a 2-handle. Note that  $H_2(\tilde{T}_n) \cong H_2(\tilde{T}_{n,l}) \cong \mathbb{Z}$ , and a generator is given by the core of the first stage of  $T_n$  (capped by a disk in  $B^4$ ).

**LEMMA 2.2.**  *$\tilde{T}_{n+1,l}$  is diffeomorphic to the handlebody obtained by gluing a 2-handle to  $B^4$  along the knot  $D^n K_l$  with framing  $-1$ .*

*Proof.* Recall that  $T_{n+1}$  is diffeomorphic to  $S^1 \times D^3$ , with attaching circle an  $(n+1)$ -fold Whitehead curve (essentially  $D^{n+1}(S^1 \times \text{point in } \partial D^3)$ ). To get  $\tilde{T}_{n+1}$ , we glue this onto a 4-ball. Equivalently, we may think of the 4-ball as a 2-handle glued to the attaching curve of  $T_{n+1}$ . Now glue on the last handle to obtain  $\tilde{T}_{n+1,l}$ . This turns  $T_{n+1} \approx S^1 \times D^3$  into a 4-ball, but puts  $l$  twists into the Whitehead curve, yielding  $D^n K_l$  as desired. QED

Figure 3 shows a Kirby calculus picture of this argument, with  $n = 0$ . The first picture shows  $\tilde{T}_1$  (with the 4-ball represented as a 2-handle). In the second picture we have added a

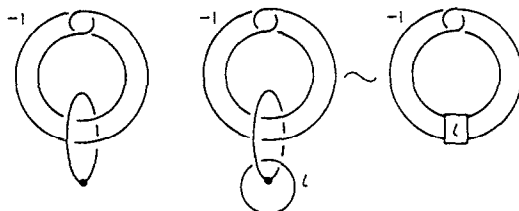


Fig. 3.

handle to get  $\tilde{T}_{1,1}$ . This handle cancels the 1-handle to yield the desired handlebody on  $K_l$ . The pictures for  $n > 0$  are similar; simply double the  $-1$ -framed curve  $n$  times in each picture. (The reader should verify that doubling commutes with the twisting.)

Now, let  $M_m = \overline{\mathbb{CP}}^2 \# (\#_m \mathbb{CP}^2)$ . Let  $e_0, e_1, \dots, e_m$  be the standard generators of  $H_2(M_m)$  (with  $e_0 \cdot e_0 = -1$ ). For convenience, let  $N \subset \mathbb{Z} \times \mathbb{Z}$  be the set of pairs  $(n, l)$  with  $0 \leq n \leq 5, l \geq 1$  or  $n = 6, l \geq 2$  or  $n = 7, l \geq 3$ .

**LEMMA 2.3.** *For  $m$  sufficiently large,  $\tilde{T}_8$  has an orientation-preserving embedding in  $M_m$  representing the class  $x = 3e_0 + \sum_{i=1}^8 e_i$ . Similarly, for each  $(n, l)$  in  $N$ ,  $\tilde{T}_{n+1,l}$  embeds in  $M_m$  (for  $m$  large) representing  $x$ . These embeddings all have 1-connected complements (except for  $\tilde{T}_{8,3}$ ).*

The proof of this (by direct construction) constitutes §3. The remainder of §2 is devoted to applications. Note that Casson's embedding theorem [1] guarantees the existence of arbitrarily large towers representing  $x$  in  $M_9$ . Thus, the difficulty in Lemma 2.3 comes from allowing only one kink at each stage.

*Proof of Theorem 2.1.* First, we show that  $x$  (in Lemma 2.3) cannot be represented by a smoothly embedded sphere. Consider the case  $m = 8$ . Now  $x \cdot x = -1$ , so  $x$  generates an orthogonal summand of the intersection form. Its complement,  $x^\perp$ , has rank = signature = 8, so it is positive definite. Furthermore,  $x$  is clearly characteristic ( $x \cdot y \equiv y \cdot y \pmod{2}$ ) for all  $y$  in  $H_2(M_8)$  so  $x^\perp$  is an even form. (In fact, it must be  $E_8$ ; see [7].) For larger values of  $m$ , we merely add  $\langle 1 \rangle$  summands to  $x^\perp$ . The  $E_8$  persists, so  $x^\perp$  is a nonstandard definite form for all  $m \geq 8$  (see [7]). But if  $x$  were represented by a smooth sphere, we could blow it down as in [5] to get a manifold with form  $x^\perp$ , contradicting Donaldson's Theorem [2].

Now pick  $(n, l)$  in  $N$  and suppose  $D^n K_l$  is slice. By Lemma 2.2,  $\tilde{T}_{n+1,l}$  is obtained by gluing a 2-handle to  $B^4$  along  $D^n K_l$ . The slice disk union the core of the 2-handle gives an embedded sphere in  $\tilde{T}_{n+1,l}$  generating  $H_2$ . By Lemma 2.3, we now obtain an embedded sphere representing  $x$ , which is impossible. Similarly, if  $k_-(D^n K_l) = 0$ , we have an immersed disk with only positive kinks spanning  $D^n K_l$ , which gives a sphere with only positive kinks representing  $x$ . We can remove these kinks by blowing up  $\mathbb{CP}^2$ 's as in [5], obtaining an embedded sphere representing  $x$  for a larger value of  $m$ . Hence,  $k_-(D^n K_l) \neq 0$ .

Now note that any double of a knot spans an obvious disk with only one kink (as does  $K_l$ ); thus,  $k(D^n K_l) = (0, 1)$ . This completes the proof for  $(n, l)$  in  $N$ . The only remaining case is  $D^7 K_2$ . This case follows from a modification of Lemma 2.3, which we discuss in section 3.12.

QED

**COROLLARY 2.4.** *The  $n$ -fold Whitehead link  $Wh_n$  is not smoothly slice for  $n \leq 7$ .*

The link  $Wh_n$  is obtained from the Hopf link by doubling one component  $n$  times. Freedman has shown that  $Wh_n$  is topologically slice for  $n \geq 4$  [4]. (For  $n \geq 5$ , see [6].)

*Proof.* Suppose  $Wh_n$  is slice for some  $n \leq 7$ . Then in particular,  $Wh_7$  is slice. By a remark of Casson [1], it follows that  $Wh_8$  may be sliced by a pair of disks  $D_1$  and  $D_2$  with  $D_1$  unknotted in  $B^4$ . (This is basically an observation of Gordon that the double of any slice disk for the unknot is itself an unknotted disk.) But  $B^4 - (\text{tubular neighborhood of } D_1) \approx S^1 \times D^3 \approx T_8$ , and  $D_2$  gives a disk spanning the attaching circle of  $T_8$ . Thus, there is an embedded sphere generating  $H_2(\tilde{T}_8)$ . Lemma 2.3 now gives a sphere representing  $x$  in  $M_m$ , but we have shown that this violates Donaldson's Theorem. QED

**COROLLARY 2.5.** *Let  $\Sigma_{n,l}$  denote the homology 3-sphere obtained by  $-1$  surgery on  $D^n K_l$ .*

For  $(n, l)$  in  $N$ ,  $\Sigma_{n,l}$  does not bound any positive definite manifold  $W$  with  $\pi_1(W) = 0$ . For  $(n, l) \neq (7, 3)$ , we may weaken the  $\pi_1$  condition to: the image of  $\pi_1(\partial W) \rightarrow \pi_1(W)$  normally generates  $\pi_1(W)$ .

Note that for  $n > 0$  (or  $l$  even),  $\Sigma_{n,l}$  has  $\mu$ -invariant zero.

*Proof.* By Lemma 2.2,  $\Sigma_{n,l}$  is the boundary of  $\tilde{T}_{n+1,l}$ . Lemma 2.3 gives an embedding of  $\tilde{T}_{n+1,l}$  in  $M_m$ . If  $\Sigma_{n,l}$  bounded a manifold  $W$  as given above, we could remove  $\text{int } \tilde{T}_{n+1,l}$  from  $M_m$ , and replace it by  $W$ . This would give a positive definite, 1-connected manifold contradicting Donaldson's Theorem. (Recall that for  $(n, l) \neq (7, 3)$ ,  $M_m - \text{int } \tilde{T}_{n+1,l}$  is 1-connected.) QED

Note that  $\Sigma_{n,l}$  actually is the oriented boundary of a nonstandard negative definite manifold, namely  $M_m - \text{int } \tilde{T}_{n+1,l}$  (with reversed orientation).

Here is a way to interpret these results. Call two homology spheres  $\Sigma_1$  and  $\Sigma_2$  equivalent if there is an oriented bordism  $V$  between them such that each inclusion  $\Sigma_i \rightarrow V$  induces a homology isomorphism and a  $\pi_1$  epimorphism (or alternatively, has image which normally generates  $\pi_1(V)$ ). Equivalence classes of homology spheres form a group under connected sum. The above remark shows that for  $(n, l) \in N - (7, 3)$ ,  $\Sigma_{n,l}$  has infinite order in this group. (In fact, any oriented connected sum of these (varying  $n$  and  $l$ ) cannot bound an acyclic manifold with  $\pi_1$  onto, since it bounds a nonstandard, negative definite, 1-connected manifold.)

### §3. PROOF OF LEMMA 2.3

We will prove the lemma by explicitly constructing the desired embeddings, one stage at a time. Thus, we may truncate the argument at any stage to obtain partial results. For example, to show that the double of the trefoil,  $DK_1$ , has kinkiness  $(0, 1)$ , it suffices to embed  $\tilde{T}_{2,1}$ .

Recall that  $\tilde{T}_8 = B^4 \cup T_8$ ,  $T_8$  the simplest 8-stage tower. We embed this as follows: First we embed  $B^4$  in  $M_m$ ,  $m$  sufficiently large. Then we embed the core of  $T_8$  (a 2-complex) in  $M_m - \text{int } B^4$ . A regular neighborhood of this will be  $T_8$ . The core will be embedded one stage at a time. For the first stage, we must construct an immersed disk  $c_1$  with exactly one kink, which represents the correct homology class  $x$ , and intersects  $\partial B^4$  in  $\partial c_1 = \text{unknot}$  in  $\partial B^4$ . A regular neighborhood of  $c_1$  will be  $k_1$ , the first stage kinky handle. Note that  $k_1$  will be attached to  $B^4$  with the correct framing, since  $x \cdot x = -1$ . The second stage core must be a disk  $c_2$  with one kink, which intersects  $c_1$  only at  $\partial c_2 = \text{a circle in } c_1$  generating  $\pi_1(c_1)$ . It will be necessary to check that the corresponding kinky handle  $k_2$  attaches to  $k_1$  with the correct framing. We must then successively construct  $c_3, \dots, c_8$ , and verify that each  $k_n$  attaches to  $k_{n-1}$  with the correct framing. This will give the desired embedding of  $\tilde{T}_8$ . Note that each kink will necessarily be negative, as required; a positive kink could be eliminated by blowing up a  $\mathbb{C}P^2$  as in [5], changing  $T_8$  to a standard 2-handle and contradicting Donaldson's theorem.

The embeddings of  $\tilde{T}_{n,l}$  will generally be visible during the above construction. We will merely need to modify  $\tilde{T}_{n+1}$  by replacing  $c_{n+1}$  by an embedded disk with suitably altered framing.

We will represent  $M_m - \text{int } B^4$  as a handlebody: one 0-handle and  $m + 1$  2-handles. The 2-handles represent the standard generators  $e_0, \dots, e_m$  of  $H_2(M_m)$ ; let  $h_i$  denote the handle representing  $e_i$ . Identify the 0-handle as  $B^3 \times I$ , with the 2-handles attached to the top face. These will attach to unlinked and unknotted circles, with framings  $\pm 1$ . (Only  $h_0$  has framing  $-1$ ). In order to scrutinize embeddings in  $B^3 \times I$ , we represent the  $I$  coordinate by time and observe pictures of successive  $B^3 \times$  point slices. We let time increase downward, away from

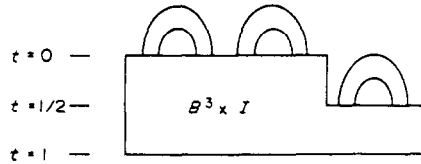


Fig. 4.

the 2-handles. For convenience, we distort the model slightly so that some 2-handles are attached at time  $t = \frac{1}{2}$ . This is shown schematically in Figure 4.

Our embedded 2-complex will intersect any given 2-handle in a disjoint union of disks parallel to the core of the handle. The boundaries of these disks will be visible at  $t = 0$  or  $\frac{1}{2}$  as a family of parallel circles, linked together by a  $\pm 1$  twist (with  $-1$  only for  $h_0$ ). We will not draw the handles themselves, but we will assume an excess of them (i.e.,  $m$  large) so that such collections of circles will always be available when necessary.

We will now begin the explicit construction. We will describe the first few stages carefully to establish the methods involved. Subsequent stages will then be relatively straightforward. A picture of the entire construction appears at the end of this section.

**3.1. Stage 1.** To construct  $c_1$ , we begin with 11 oriented disks: three in  $h_0$  and one each in  $h_1, \dots, h_8$ . (We attach  $h_0, \dots, h_4$  at  $t = 0$ , and  $h_5, \dots, h_8$  at  $t = \frac{1}{2}$ .) The rest of  $c_1$  will lie in the 0-handle, so it will represent the correct homology class  $x = 3e_0 + \sum_{i=1}^8 e_i$ . The part of  $c_1$  in the 0-handle is shown in Fig. 5. This depicts seven different instants of time, with the pictures ordered from left to right. In the first picture,  $t = 0$ , we see the oriented boundaries of the disks in  $h_0, \dots, h_4$ . As time increases, these are joined together by bands (1-handles) which respect the orientations.

The second picture shows the resulting circle, which isotopes to the left-handed trefoil in the third picture. As time continues to increase, the knot pushes through itself at  $t = \frac{1}{4}$  to become an unknot. This creates the kink in  $c_1$ , depicted as a large dot in the center picture. At  $t = \frac{1}{2}$ , the boundaries of the remaining disks appear and trivially band into the circle. We are then left with an unknot at  $t = 1$  as required.

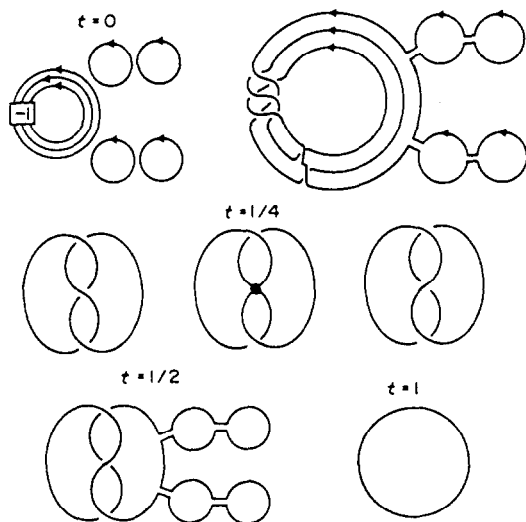


Fig. 5.

Note that the complement of  $c_1$  is 1-connected. To see this, observe that a disk in (for example)  $h_8$  bounds a meridian at  $t = \frac{1}{2}$ , due to the  $+1$  twist in the attaching map. In fact, this gives an embedded  $S^2$  which intersects  $c_1$  exactly once. We will call such an object a *Norman sphere* for  $c_1$ , after [8]. Note that this Norman sphere has a twisted normal bundle. We obtain 8 such disjoint spheres from  $h_1, \dots, h_8$ .

### 3.2. The attaching circle for stage 2

We must choose carefully the framed circle in  $\partial k_1$  to which we will attach  $k_2$ . Now  $k_1$  is a regular neighborhood of  $c_1$ ; at the time  $t = \frac{1}{4}$  (the center picture of Fig. 5)  $k_1$  appears as in Fig. 6. The dashed curve appearing on the boundary is the desired circle. Note that this circle generates  $\pi_1(k_1)$ , and it is obtained from an embedded circle in  $c_1$  by pushing out to  $\partial k_1$ . Thus, attaching  $k_2$  along this curve will yield a 2-stage tower, provided that the framing is correct.

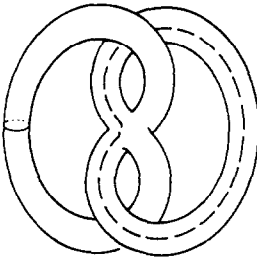


Fig. 6.

The correct framing is the one induced by time; i.e., one vector field is tangent to the surface at  $t = \frac{1}{4}$  formed by  $\partial k_1$ . To prove this, we use the following fact: Attaching a 2-handle to the correct framed curve transforms  $(k_1, \partial c_1)$  into  $(B^4, \text{unknot})$ , whereas the incorrect framing results in  $(B^4, \text{nontrivial knot})$ . Our strategy is to abstractly attach a 2-handle  $h$  along the indicated framed curve, then to isotope an unknot onto  $\partial c_1$  within  $\partial(k_1 \cup h)$ .

Choose a time  $t_0 < \frac{1}{4}$ , corresponding to the third picture of Fig. 5. If we restrict attention to  $t \leq t_0$  and handles  $h_0, \dots, h_4$ , then  $c_1$  restricts to an embedded disk, and  $k_1$  restricts to a regular neighborhood of this. Push the disk straight out to  $\partial k_1$ , preserving the  $t$  coordinate near  $t_0$ . The circle  $C$  bounding the disk now is clearly an unknot in  $\partial k_1$  (and will remain unknotted when we add  $h$ ). Figure 7 shows the circle  $C$ . (The number of meridinal twists will not concern us.)

We isotope  $C$  by letting  $t$  increase. Figure 8 shows  $t = \frac{1}{4}$ . Note that we cannot carry this

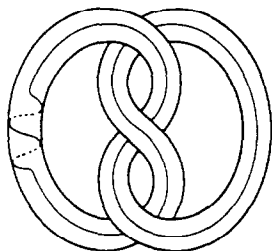


Fig. 7.

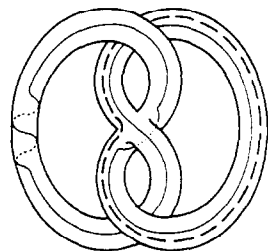


Fig. 8.

isotopy much farther, because of problems which occur near the kink of  $c_1$ . We use the 2-handle  $h$  to correct these problems.

Note that an arc of  $C$  runs parallel to the attaching curve of  $h$  (the dashed curve). If we imagine  $h$  to be abstractly attached here, we may slide this arc over  $h$  (in  $\partial(k_1 \cup h)$ ). Figure 9 shows a neighborhood of the kink. The handle slide is portrayed in the first two pictures. Crosshatching indicates the arc of  $C$  which has been slid over  $h$ . We have used the fact that  $h$  is attached via the framing induced by  $t$ ; any other framing would cause twisting here involving the time coordinate.

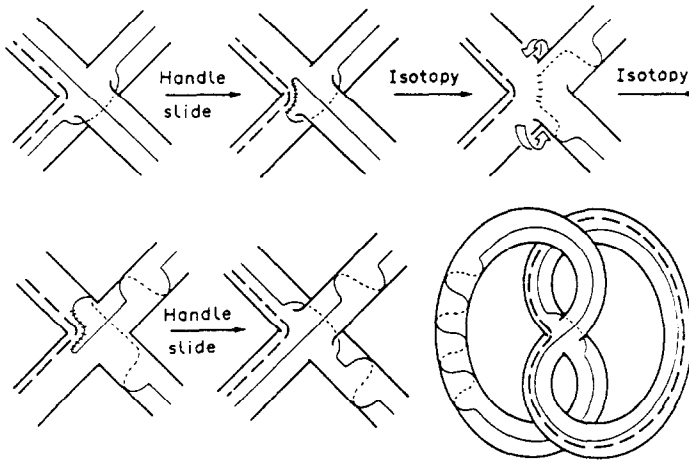


Fig. 9.

In the next two pictures, the crosshatched arc is slid  $360^\circ$  around a vertical circle, as indicated by the arrows. This twists the rest of  $C$  around  $k_1$ . We then slide the arc back over  $h$ . The result is shown in the last picture: We have reversed the crossing near the kink of  $c_1$  (and added several meridinal twists to  $C$ ).

We next isotope  $C$  by increasing  $t$  to  $\frac{3}{8}$ . Now  $k_1$  appears as an unknotted solid torus, with  $C$  a (twisted) longitude in the boundary. When we restrict our attention to the remainder of the ambient space ( $t \geq \frac{3}{8}$  and  $h_5, \dots, h_8$ )  $c_1$  becomes an embedded annulus and  $k_1$  restricts to a regular neighborhood of this. Thus, we may slide  $C$  all the way down to  $t = 1$ , where it still appears as a longitude of a solid torus. (The twisting changes when we go over  $h_5, \dots, h_8$ .) The entire solid torus at  $t = 1$  lies in  $\partial k_1$ , so we may isotope  $C$  to the core circle, which is  $\partial c_1$ . Hence,  $\partial c_1$  is indeed unknotted in  $\partial(k_1 \cup h)$ . This completes the proof that we have chosen a correct framed curve for attaching  $k_2$ .

**3.3. Stage 2.** In this section we describe the embedding of  $c_2$ . The techniques developed here will also be used for most of the higher stages.

Note that at  $t = \frac{1}{4}$  there is an embedded disk bounding the required circle with the correct framing; see Fig. 10. Unfortunately, this disk intersects  $k_1$ . We fix this with the *Norman trick* (as in [8]). Recall, from section 3.1, the Norman sphere for  $c_1$  associated with handle  $h_1$ . We tube this into the given disk, obtaining a new disk  $D$  disjoint from  $k_1$  (except along  $\partial D$ ). Since the Norman sphere represents the homology class  $e_1$ , and  $e_1 \cdot e_1 = +1$ , the framing induced by  $D$  will be off by  $+1$  twist from the desired one. Thus, thickening  $D$  gives us an embedding of  $\tilde{T}_{1,1}$ .

It is now easy to embed  $\tilde{T}_{1,l}$  for  $l \geq 2$ . To do this, locate  $l - 1$  disjoint spheres representing  $e_9, \dots, e_{l+7}$  and tube these into  $D$ , obtaining a new disk with framing off by  $l$  twists. In

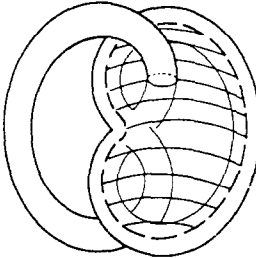


Fig. 10.

general, it is always easy to increase framings in this setting, but difficult to decrease them. For example, an embedding of  $\tilde{T}_{n,l}$  automatically gives embeddings of  $\tilde{T}_{n,l'}$  for  $l' \geq l$ .

To embed  $\tilde{T}_2$ , it is necessary to decrease the framing of  $D$ , at the expense of adding a kink. We do this via a trick of Casson [1]. Let  $\tau_1$  be the distinguished torus of stage 1; this is embedded near the kink of  $c_1$  and intersects  $D$  exactly once. There is a circle  $C_1$  in  $\tau_1$  which is a meridian of  $c_1$ . Use the Norman sphere for  $c_1$  representing  $e_2$  to make  $C_1$  bound a disk with interior disjoint from  $c_1$ ,  $D$ , and  $\tau_1$ . Now use this disk to ambiently surger  $\tau_1$  into a sphere  $S$ . Because the Norman sphere has a twisted normal bundle, the two “parallel” disks used in surgery actually intersect each other once. Thus,  $S$  has a single kink. Note that  $S$  and  $\tau_1$  represent the same class in  $H_2(M_m - \text{int } \tilde{T}_1, \partial \tilde{T}_1)$ .

Now  $S$  intersects  $D$  exactly once. We form the connected sum  $D \# S$  as follows: Let  $B$  be a small 4-ball centered at the intersection point, such that  $D$  and  $S$  intersect  $B$  in a standard pair of transverse disks. Remove these disks, and replace them by an annulus spanning the Hopf link in  $\partial B$ . Choose the annulus so that  $D \# S$  represents the relative homology class  $[D] - [S]$  when  $D$  and  $S$  are oriented so that  $[D] \cdot [S] = +1$ . Now the relative homological self-intersection number of  $D \# S$  (defined relative to the standard framing given in section 3.2) is given by  $[D \# S]^2 = ([D] - [S])^2 = [D]^2 - 2[D] \cdot [S] + [S]^2 = 1 - 2 + 0 = -1$ . Thus, if the immersed disk  $D \# S$  is thickened to a kinky handle, its framing will be off by  $-1$ . We easily correct this by tubing  $S$  into a sphere  $S'$  representing  $e_9$ . The disk  $D \# S \# S'$  is the desired  $c_2$ .

We show that  $M_m - \tilde{T}_2$  is 1-connected: Any loop  $\gamma$  in this space bounds an immersed disk in  $M_m - B^4$ . We make the disk disjoint from  $c_2$  by finger moves, pushing each intersection across  $\partial c_2$  into  $c_1$ . Now remove intersections with  $c_1$ , using copies of the Norman sphere representing  $e_8$ . We now have the required null homotopy for  $\gamma$  in  $M_m - \tilde{T}_2$ . The same argument works for  $\tilde{T}_{1,l}$ . In fact, it will work for all of our constructions through  $\tilde{T}_{6,l}$  and  $\tilde{T}_7$ . We omit further reference to this at these stages. Stage 8 requires further comment, however, because the Norman sphere for  $e_8$  is used in its construction.

**3.4. A Picture of Stage 2.** A neighborhood of the kink in  $c_1$  is depicted in Fig. 11, with the distinguished torus  $\tau_1$  shown (dashed curves). Time increases, as usual, from left to right. The

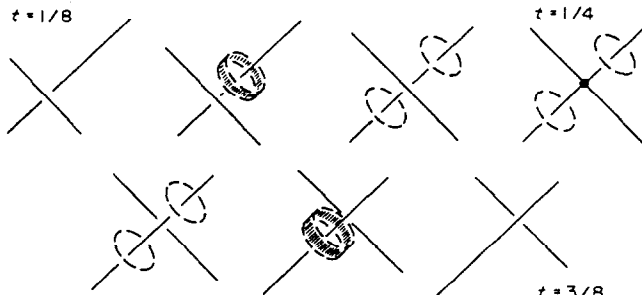


Fig. 11.

torus first appears as an annulus around one sheet of  $c_1$ . This splits into two circles which separate around the other sheet of  $c_1$ , then converge into another annulus. Thus,  $\tau_1$  contains meridians to both sheets of  $c_1$ .

We next ambiently surgery on the circle  $C_1$  to obtain  $S$ . We choose  $C_1$  to be a meridian in the initial annulus of  $\tau_1$ . The surgery disk runs from  $C_1$  over the handle  $h_2$ . This is evident in our picture of  $S$ , Fig. 12. At  $t = 0$ , we see the boundaries of two parallel disks in  $h_2$ . As time increases, these become meridians of the trefoil knot formed by  $c_1$ . The kink in  $c_2$  occurs in the fourth picture, as the two meridians unlink from each other. We have now described the two “parallel” copies of the surgery disk. Shortly after  $t = \frac{1}{8}$ , these disks merge into  $\tau_1$  (from which the interior of the initial annulus has been removed). Compare the last three pictures with Fig. 11.

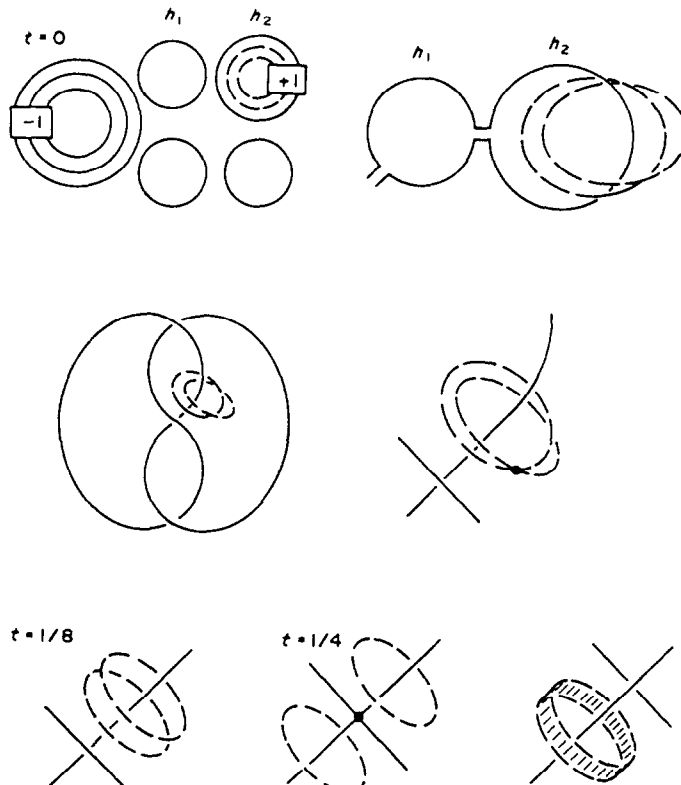


Fig. 12.

We also need a picture of the tubing operation used to form  $D \# S$ . Before tubing,  $D$  and  $S$  intersect transversely as in Fig. 13. We now delete a small disk from each surface. (This removes a small segment from each arc in Fig. 13.) Next, we connect the boundary circles by a

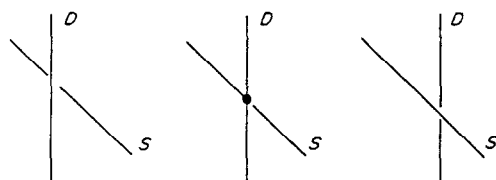


Fig. 13.

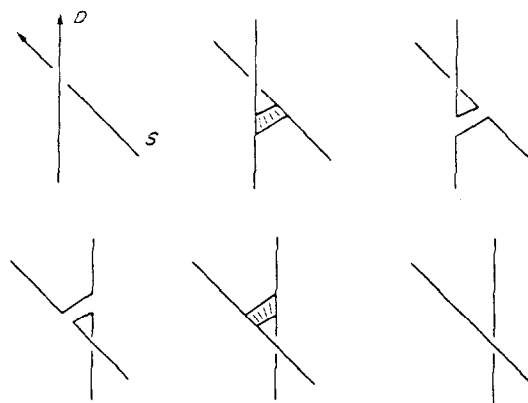


Fig. 14.

small annulus, i.e., a 1-handle and 2-handle. This is shown in Fig. 14. The 1-handle is visible in the second picture, the 2-handle is in the fifth. Note that if  $D$  and  $S$  are oriented so that  $[D] \cdot [S] = +1$  (as in the figure) the resulting surface represents  $[D] - [S]$  as desired. (To realize  $[D] + [S]$  put a right half-twist in the 1-handle.)

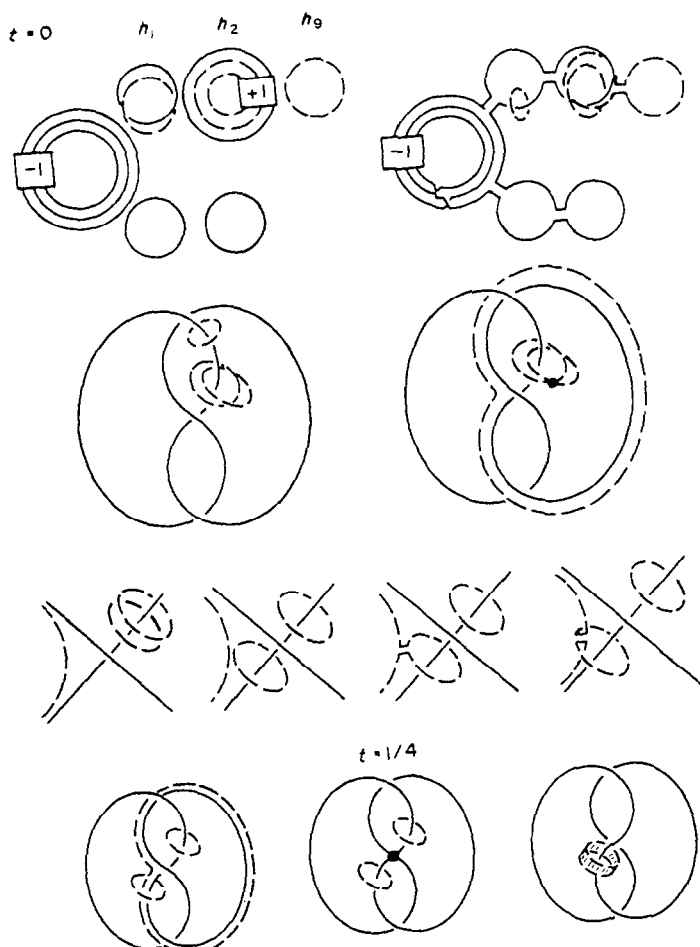


Fig. 15.

The reader is encouraged to draw Fig. 14 with a parallel copy, and notice that two left-handed twists are introduced by this procedure. This is the geometric realization of the algebra in section 3.3 which corrected a framing problem via the term  $-2[D] \cdot [S]$ .

A complete picture of  $c_2$  is given in Fig. 15. The sphere  $S$  is clearly visible. The disk running over  $h_9$  corresponds to the sphere  $S'$ . This tubes into  $S$  in the second picture. The disk  $D$  is also visible: The Norman sphere begins with a disk in  $h_1$ , then shrinks to a meridian in the second picture. This meridian continues into the third picture where it tubes into the original disk from which  $D$  was constructed (Fig. 10). We have perturbed this disk into general position with respect to time. Thus, we see the meridian gradually expanding until it gets close to the attaching circle (in the fourth picture). In subsequent pictures,  $D$  tubes into  $S$  (as described above), then merges with  $c_1$  along the correct circle at  $t = \frac{1}{4}$ .

We showed in section 3.3 that the natural framing of the attaching circle of  $k_2$  agreed with the framing specified in 3.2. This may also be verified directly from the picture: Construct a parallel copy of  $c_2$ . At any generic time, this looks like a framing on each circle of  $c_2$ . Each disk inside a handle results in one twist, thus at  $t = 0$  we have a total of +4 twists. Two of these twists are eliminated at the tube between  $S$  and  $D$  (as described previously). The other two are compensated for by the (negative) kink in  $c_2$ . (Recall that we use homology to define framings on kinky handles; thus,  $[c_2] \cdot [c_2] = \chi(v) + 2 \text{ self } c_2 = 2 - 2 = 0$ , as required.) Details are left to the reader.

**3.5 The attaching circle for stage 3.** We now describe the framed circle in  $\hat{c}k_2$  to which we attach  $k_3$ . The results of this section will also be useful at later stages, in particular, whenever the kink of the previous stage comes from surgery on a distinguished torus. For this reason, we give several variations of the framed circle.

The fine curves in Fig. 16 represent an annulus  $A$  with boundary components  $\partial_0 A$  and  $\partial_1 A$ . The circle  $\partial_0 A$  lies in  $c_2$ , and  $\partial_1 A$  is the circle visible in the last picture. Note that  $\partial_0 A$  runs through the kink of  $c_2$ , hence, generates  $\pi_1(c_2)$ . (It is visible in subsequent pictures as a pair of points; these are joined by an arc in the fifth picture.) The annulus  $A$  intersects  $\hat{c}k_2$  in a suitable circle. We specify the framing on this by framing all of  $A$ . This is achieved by framing  $\hat{c}_1 A$  in the last picture. (The normal bundle of  $\hat{c}_1 A$  in the slice  $t = \text{constant}$  is the restriction of the normal bundle of  $A$  to  $\hat{c}_1 A$ .) In fact, the 0-framing on  $\hat{c}_1 A$  is correct.

Once we have shown this, we may construct other suitable framed curves as follows: Near  $t = \frac{1}{4}$  in Fig. 16, give one circle a  $360^\circ$  twist, then join the circles together as before. This gives a self-diffeomorphism of  $k_2$ ; hence, it sends the above framed curve to another suitable one. A possible result is shown in Fig. 17. Note that in the third picture, a twist is introduced in the framing of the annulus. Thus, the correct framing on  $\partial k_2$  corresponds to framing  $-1$  on the circle in the last picture.

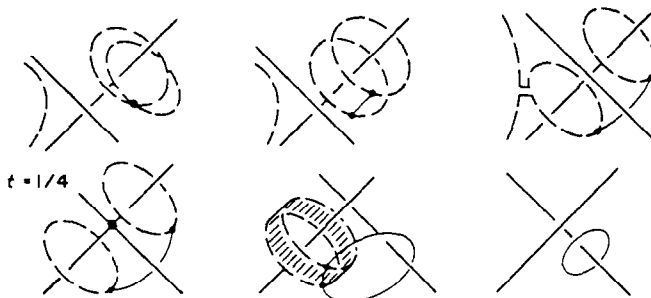


Fig. 16.

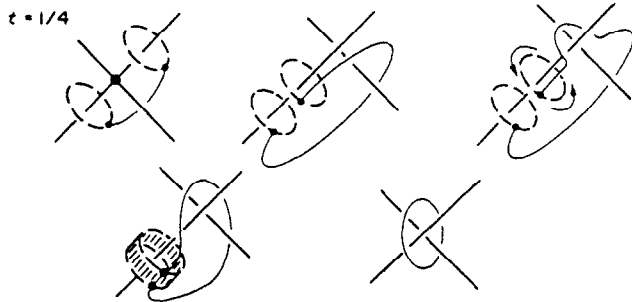


Fig. 17.

Figure 18 shows a similar variation. This time we twist the circle in the opposite direction, but the correct framing on the meridian in the last picture is still  $-1$ . The difference between Fig. 17 and 18 is that in the latter case, the annulus passes through  $c_1$ . (Note that in the absence of  $c_1$ , the framing may be changed by 2 simply by throwing an arc of the annulus over one of the circles.) In practice, we must remove the intersection point with a Norman sphere for  $c_1$ . The  $+1$  twist in the normal bundle of the Norman sphere will cancel the  $-1$  twist in the annulus, so we will be left with a 0-framed meridian like in Fig. 16.

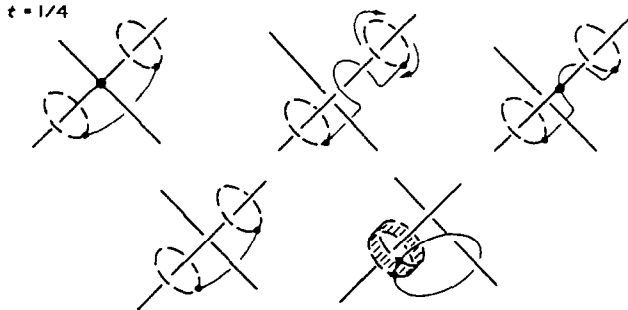


Fig. 18.

To see that the 0-framing in Fig. 16 is correct, recall that by construction  $c_2 = D \# S \# S'$ . Let  $S_-$  denote  $S$  with a small puncture. There is an ambient isotopy (moving  $\partial c_2$ ) which sends  $c_2$  onto  $S_-$ . (First shrink away  $D$ , sending  $c_2$  onto  $S_- \# S'$ , then use the puncture to slip the surface off of  $h_9$ .) We may assume that this isotopy fixes (pointwise) a neighborhood of the annulus  $A$ . (Note that  $A$  does not separate  $c_2$ .) We may also locate the puncture of  $S_-$  at any convenient place on  $S$ . Since  $k_2$  is a regular neighborhood of  $c_2$ , the isotopy sends  $k_2$  to a regular neighborhood  $N(S_-)$ . The circle  $\partial c_2$  in  $\partial k_2$  is sent to  $\partial S_-$  in  $\partial N(S_-)$ . It is now sufficient to attach a 2-handle  $h$  to  $N(S_-)$  along the framed curve in  $\partial N(S_-)$  determined by  $A$ , then to show that  $\partial S_-$  bounds an embedded disk in  $\partial(N(S_-) \cup h)$ . (Compare with section 3.2.)

Figure 19 shows  $N(S_-)$ . (Compare with our picture of  $S$ , Fig. 12.) Stage 1 has been erased. The two solid tori at  $t = 0$  are the attaching regions of 2-handles in  $h_2$ . These pass through each other as time increases, exposing the annulus  $A$  (fine curve). The puncture of  $S_-$  has been put in the final annulus of  $S$  (last picture of Fig. 12); thus our last picture shows a neighborhood of a punctured annulus. The dotted curve in the boundary indicates where a 2-handle should be added to get back a neighborhood of the entire annulus; this is the curve  $\partial S_-$ .

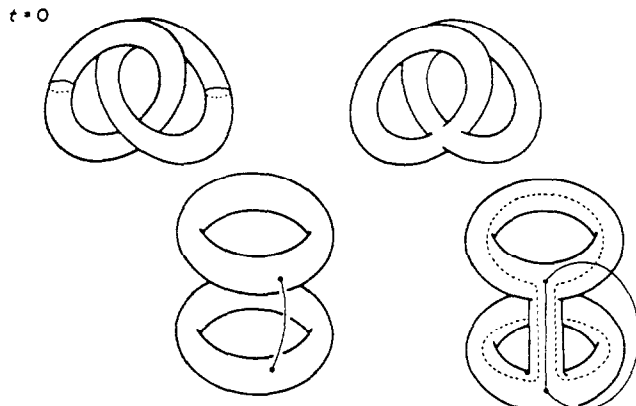


Fig. 19.

The 2-handle  $h$  can now be added ambiently. (It will hit stage 1, but this does not concern us now.) Simply turn the annulus  $A$  into a disk by spanning  $\partial_1 A$ , the fine circle in the last picture of Fig. 19, with the obvious disk. Taking a regular neighborhood gives a 2-handle  $h$  realizing the correct framing (0-framing in the last picture). To draw  $h$ , simply flatten the curves representing  $A$ , then cancel the extra 1-handle in the last picture. The result (up to isotopy) is shown in Fig. 20. (The third picture comes from the second by isotopy.) Figure 21 now shows the required disk bounding  $\partial S_-$ . The two circles at  $t = 0$  bound disks in the boundaries of the 2-handles in  $h_2$ . In the third picture, these are connected by a 1-handle. The resulting boundary isotopes to  $\partial S_-$ .

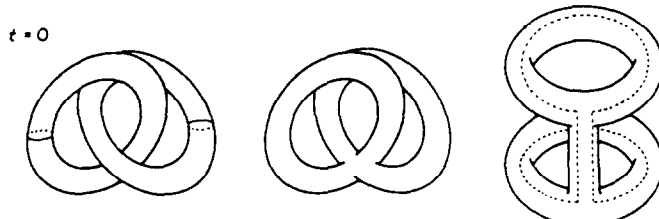


Fig. 20.

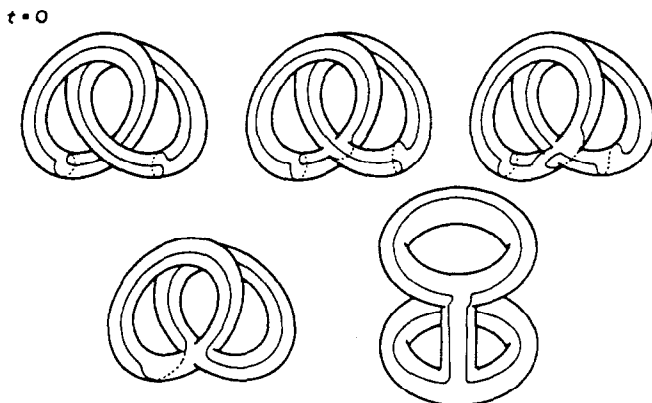


Fig. 21.

**3.6 Stage 3.** This is quite similar to Stage 2. As remarked previously, we may easily cap the attaching circle of Stage 3 by a disk with the correct framing. (Just fill in the meridian shown in Fig. 16.) The disk intersects  $c_1$  once; remove this with the Norman sphere for  $c_1$  representing  $e_3$ . We now have an embedding of  $\tilde{T}_{2,1}$  (and therefore  $\tilde{T}_{2,l}$ ,  $l \geq 1$ ). (We have thus proven our results about  $DK_l$ ,  $l \geq 1$ .) We again correct the framing via a distinguished torus. This time we use the torus  $\tau_2$ , near the kink of  $c_2$ . We surger this to an immersed sphere via the Norman sphere for  $c_2$ , which runs over the handle  $h_9$  (observe this in Fig. 15). Tubing into a sphere representing  $e_{10}$  completes the framing correction.

See Fig. 22 for a complete picture of  $c_3$ . (Compare this with Fig. 15). Note that we have made an additional modification shortly after  $t = \frac{1}{4}$ . We have twisted the attaching circle as in section 3.5 (Fig. 18). We have removed the resulting intersection with  $c_1$ , using the Norman sphere representing  $e_4$ . As remarked in section 3.5, this cancels the left twist which was introduced. Thus, the framing of  $k_3$  has not been disturbed. This modification appears pointless, but will actually be useful when we construct Stage 4.

**3.7 Stage 4.** For a picture of  $c_4$ , we refer the reader to Fig. 24, the big diagram at the end of section 3. In particular,  $t < \frac{1}{2}$  (the first page of Fig. 24) covers all of  $c_2$ ,  $c_3$  and  $c_4$  (as well as the attaching circle of  $c_5$ ).

The framed attaching circle looks just like that of  $c_3$  (the basic version—Fig. 16). The same argument shows that the 0-framing is correct. This time, however, the obvious disk intersects  $c_2$  (not  $c_1$ ). Since  $c_2$  has no remaining Norman sphere, we resort to another trick of Casson: A small distinguished torus  $\tau'_1$  for  $c_1$  hits  $c_2$  exactly once. Surger  $\tau'_1$  to an immersed sphere via  $e_4$  (as usual), then tube this into the disk to remove the intersection with  $c_2$ . This does not affect the framing since  $\tau'_1$  is disjoint from the disk. Recall that we have already used a Stage 1 torus  $\tau_1$  to construct  $c_2$ . These two tori interfere slightly. In particular, there is tangling between the attaching circles of Stages 3 and 5. This is corrected by our trick at Stage 3 involving  $e_4$  (as shown immediately after  $t = \frac{1}{4}$  in the picture of  $c_4$ ).

**3.8 Stage 5.** Since  $c_4$  has no obvious Norman sphere, the torus  $\tau_4$  is unusable. Thus, we must change our tactics for  $c_5$ . We twist the attaching circle in the manner of Fig. 17. This introduces a  $-1$  twist which we remove by tubing into a sphere representing  $e_{11}$ . (The handles  $h_{11}$ ,  $h_{12}$  and  $h_{13}$  are attached at  $t = \frac{1}{2}$ ). The details are shown in Fig. 24; note the change of notation for  $c_5$  at  $t = \frac{1}{2}$ . The attaching circle for  $c_5$  forms a Whitehead link with  $c_1$  (at  $t = \frac{1}{2}$  and the following picture—the reader should verify this isotopy). This persists without change until  $t = \frac{3}{4}$ , where  $c_5$  pulls through itself, generating a kink. The link has now become unlinked; we close  $c_5$  with a 2-handle just before  $t = 1$ . (Note that at  $t = \frac{3}{4}$  the 0-framing of  $c_5$  changes to  $+2$ , due to the compensating twists for the clasp. This corrects for the (negative) kink.)

It is not obvious that  $c_4$  or  $c_5$  can be replaced by embedded disks with twisted framings. We embed  $\tilde{T}_{3,1}$  and  $\tilde{T}_{4,1}$  by the following trick: Stage 3 could have been constructed by the method which we used for Stage 5. We could have then constructed Stages 4 through 6 by the procedure which we will use for Stages 6 through 8. (Thus the embedding would look identical for  $t \geq \frac{1}{2}$ , but each stage would be two stories lower.) The new cores of Stages 4 and 5 would then be identical to the actual cores  $c_6$  and  $c_7$ . We will show that these may be replaced by embedded disks as desired.

**3.9 Stage 6.** Isotope  $c_5$  onto the part of  $c_5$  at  $t \geq \frac{5}{8}$ . Let  $N$  be the ambient space for  $t \geq \frac{5}{8}$ , with an open regular neighborhood of  $c_1$  deleted. Thus,  $N$  is clearly diffeomorphic to  $S^1 \times D^3$ . At  $t = \frac{5}{8}$ ,  $c_5$  wraps around this in a Whitehead curve. Our pictures of  $c_5$  at  $t \geq \frac{5}{8}$  are the same as

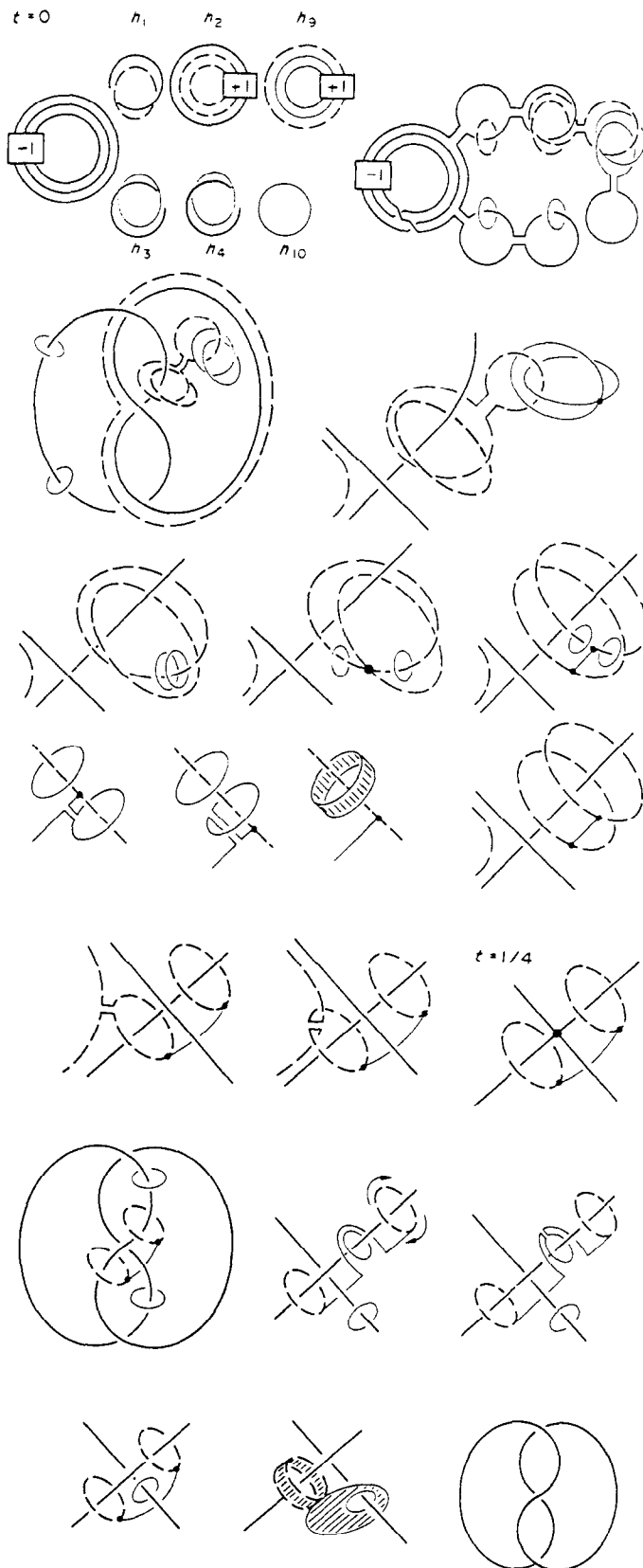


Fig. 22

those of the core of the kinky handle  $k \approx S^1 \times D^3$  shown in Fig. 23. Hence,  $(N, c_5) \approx (k, \text{core})$ ,  $N$  is a regular neighborhood of  $c_5$ , and standard kinky handle theory shows that a 0-framed meridian of  $c_1$  is a suitable attaching curve for  $c_6$ . In Fig. 24, this meridian is visible just before time  $t = \frac{3}{4}$ , when it merges into  $c_5$ .

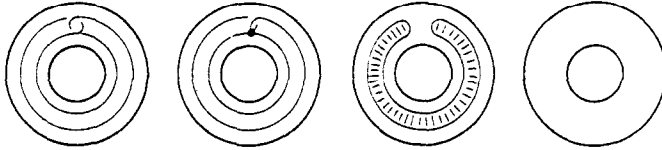


Fig. 23.

We now construct  $c_6$  in the usual way: First obtain  $\tilde{T}_{5,1}$  by tubing into the Norman sphere representing  $e_5$ . Then correct the framing with the torus  $\tau_5$  (surgered over  $h_{11}$ ) and the  $e_{12}$  sphere.

**3.10 Stage 7.** The attaching curve is standard (twisted as in Fig. 17). The resulting circle links  $c_5$  and  $c_1$  as Borromean rings. We unlink this with two Norman spheres for  $c_1$ ; see the last four pictures of Fig. 24. The Norman spheres change the framing from  $-1$  (due to the twist in the attaching circle) to  $+1$ . Thus, we have embedded  $\tilde{T}_{6,1}$ . We correct, as usual, with a distinguished torus  $\tau_6$ .

**3.11 Stage 8.** We begin with the usual (untwisted) attaching curve, a 0-framed meridian of  $c_6$ . Note that  $c_6$  has no remaining Norman spheres. Instead, we tube into a sphere representing  $e_5$ , which intersects both  $c_6$  and  $c_1$ . We remove the intersection with  $c_1$ , using the  $e_8$  Norman sphere for  $c_1$  (see  $t = \frac{2}{3}$ ). We have now introduced two twists in the framing, so we have an embedding of  $\tilde{T}_{7,2}$ . Fortunately, the distinguished torus technique is capable of cancelling two twists; simply forget the extra sphere which was used on previous occasions.

Recall, from Section 3.3, the argument that  $\tilde{T}_n$  has 1-connected complement. The argument fails for  $\tilde{T}_8$ , since we have used up all Norman spheres for  $c_1$ . We may easily correct this, however. Given a disk bounding a loop  $\gamma$ , first remove intersections with  $\tilde{T}_2$ , as we did previously. The disk now runs over  $h_8$  many times, so we have introduced intersections with  $c_8$ . Next, push all intersections with  $\tilde{T}_8$  down to  $c_3$  by finger moves. We may now remove these intersections using the Norman sphere for  $c_3$  (representing  $e_{10}$ ). Our disk is now disjoint from  $\tilde{T}_8$ . Thus,  $\tilde{T}_8$  (and similarly  $\tilde{T}_{7,2}$ ) has 1-connected complement.

**3.12 Stage 9.** We conclude section 3 by discussing embeddings of  $\tilde{T}_{8,1}$ . (These are not drawn in Fig. 24.) The attaching circle for the new disk is a 0-framed meridian of  $c_7$  (by the usual argument). Since  $c_7$  has no Norman sphere left, we use a sphere representing  $e_6$ , introducing an intersection with  $c_1$ . Remove this via a sphere for  $e_3$ . The resulting intersection with  $c_3$  can be eliminated by the Norman sphere representing  $e_{10}$ . We have now obtained an embedding of  $\tilde{T}_{8,3}$ . The complement is unlikely to be 1-connected, since there are no remaining Norman spheres. However, if we also tube the top stage into a sphere representing  $e_{14}$ , we obtain an embedding of  $\tilde{T}_{8,4}$  which has a Norman sphere for the top stage. This has 1-connected complement. (Given a disk bounding  $\gamma$ , remove it from  $\tilde{T}_8$  as before, then separate it from the top stage via the Norman sphere.)

Finally, we show how to prove Theorem 2.1 for  $D^7 K_2$ , without an embedding of  $\tilde{T}_{8,2}$ . Tube  $c_1$  into a sphere representing  $e_{15}$ . This gives an embedding of a manifold  $\tilde{T}_8$ , representing the homology class  $x + e_{15}$ . The manifold  $\tilde{T}_8$  is constructed the same way as  $\tilde{T}_8$ ,

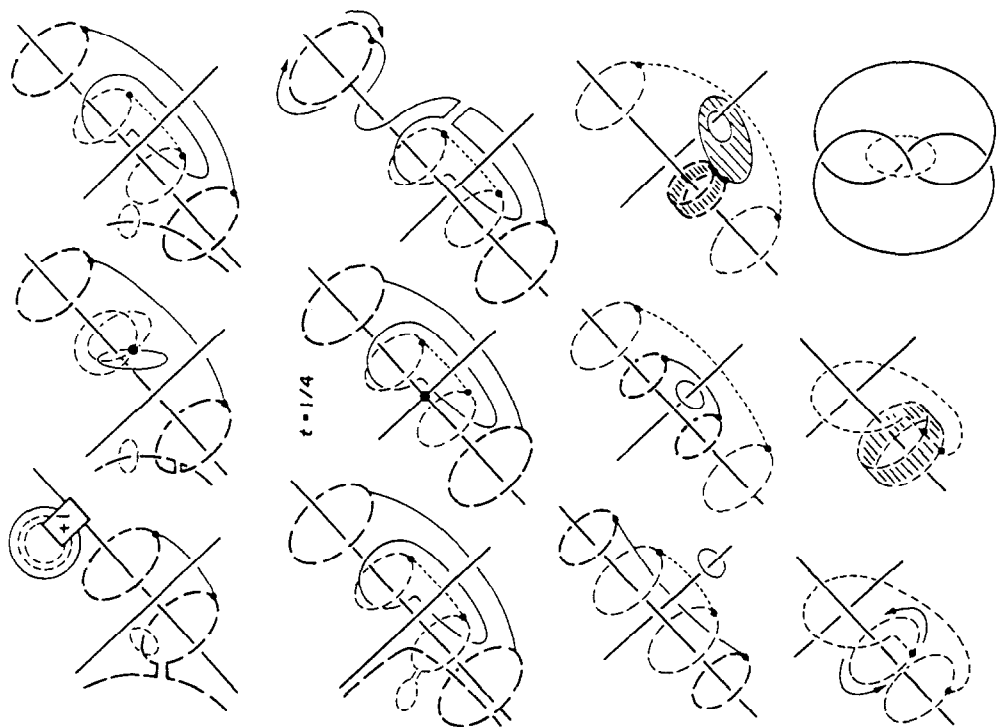


Fig. 24(ii).

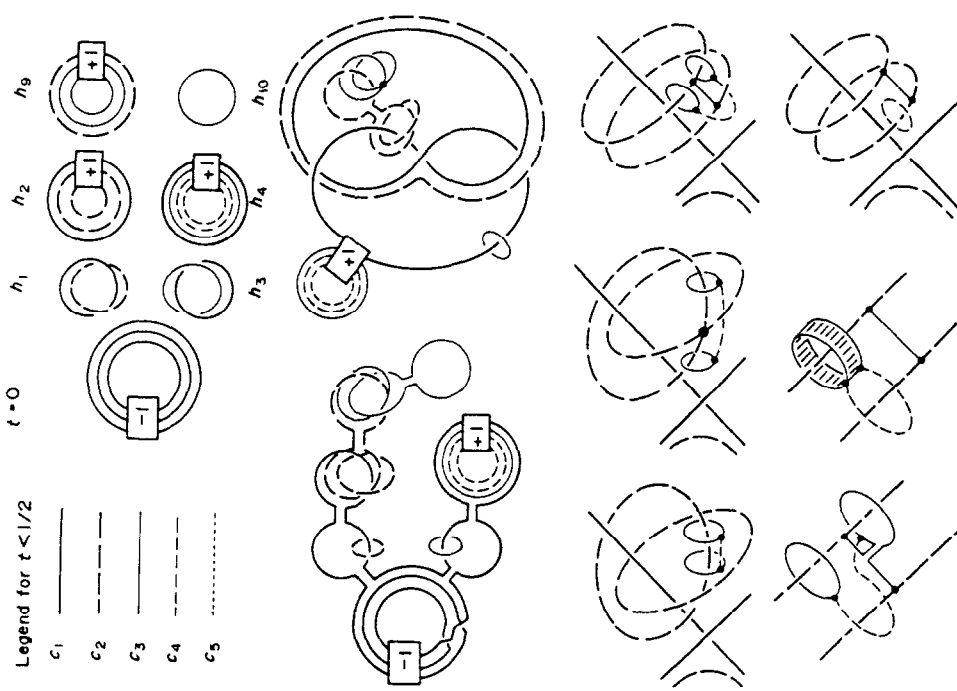


Fig. 24(i).

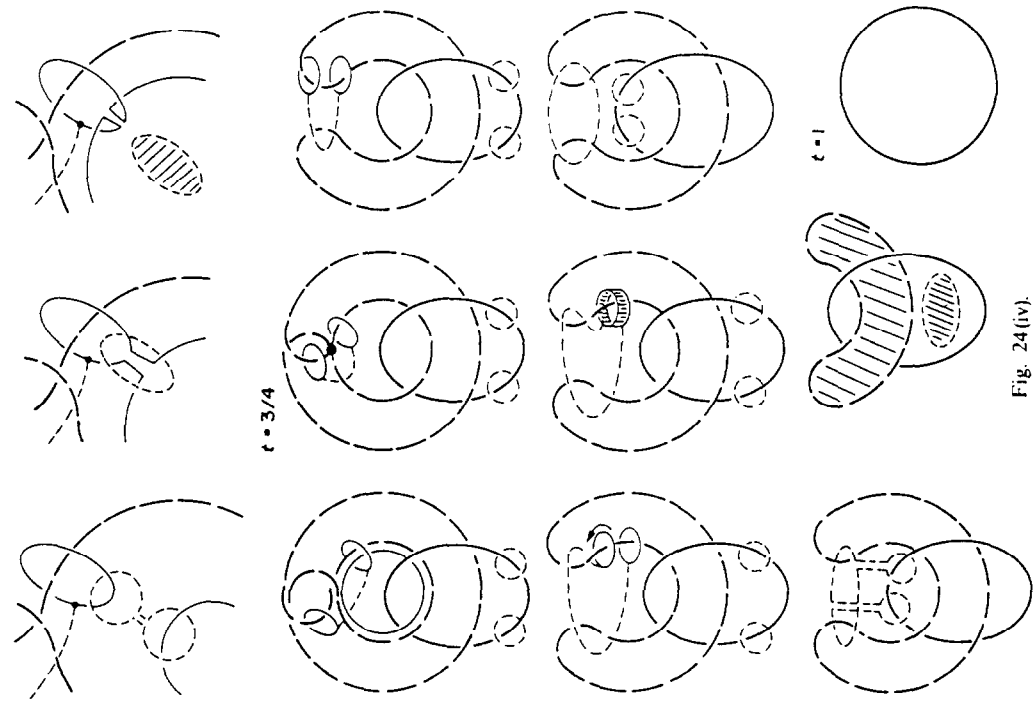


Fig. 24(iv).

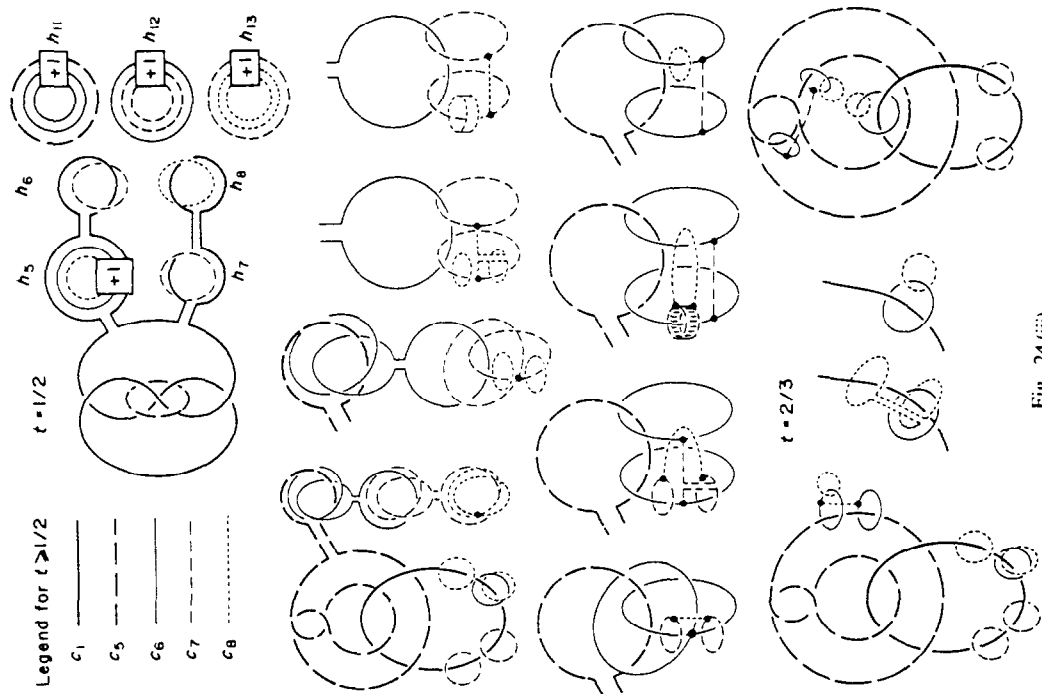


Fig. 24(iii).

Legend for  $t > 1/2$

- $c_1$  ———
- $c_5$  - - -
- $c_6$  - - -
- $c_7$  - - -
- $c_8$  - - -

except that  $T_8$  is glued to  $B^4$  with framing 0. We cap  $\bar{T}_8$  with a disk with framing 2, and call the result  $\bar{T}_{8,2}$ : Simply tube into the  $e_6$  sphere (as for  $\bar{T}_{8,3}$ ), and remove the intersection with the first stage via  $e_{15}$ . The result has 1-connected complement, due to the Norman sphere for  $c_3$  representing  $e_{10}$ . Now as in section 2, if the knot  $D^7K_2$  were slice, we would obtain an embedded sphere  $S$  in  $\bar{T}_{8,2}$  representing  $x + e_{15}$ . Furthermore, a meridian of  $S$  could be homotoped into  $\partial\bar{T}_{8,2}$  in  $\bar{T}_{8,2} - S$ . This implies that  $M_m - S$  is 1-connected. Surgery on  $S$  now contradicts Donaldson's theorem.

#### §4. CONCLUDING REMARKS

It seems likely that with some clever tricks, several more stages could be inserted into the tower of section 3. This, of course, would sharpen the results in section 2. A more interesting question is this: Can the procedure be continued indefinitely? The main defect of our method is that each stage uses up more Norman spheres than it creates (with the notable exception of Stage 5, which adds one). Thus, we need either (1) a method without this defect, or (2) settings in which we can start Stage 1 with arbitrarily large numbers of Norman spheres. The ultimate conjecture in this context is that no  $\bar{T}_n$  or  $\bar{T}_{n,l}$  ( $l \geq 1$ ) has an embedded sphere (or immersed sphere with only positive kinks) generating its homology. This would imply, for example, that no iterated double of  $K_l$  ( $l \geq 1$ ) is smoothly slice.

Another line of inquiry would be to try to attach the top stage embedded disks to framed curves which are knotted in  $\partial T_n$ . The effect of this would be to replace  $K_l$  in section 2 by the twisted double of the given knot. An interested reader is invited to experiment with these ideas.

#### REFERENCES

1. A. CASSON: Three lectures on new constructions in 4-dimensional manifolds, notes prepared by L. Guillou, Prépublications Orsay 81T06.
2. S. DONALDSON: An application of gauge theory to four-dimensional topology *J. Diff. Geometry* **18** (1983), 279–315.
3. M. H. FREEDMAN: The topology of four-dimensional manifolds *J. Diff. Geometry* **17** (1982), 357–453.
4. M. H. FREEDMAN: Slicing  $Wh_4$ . *Austin, Texas Lecture Notes*, 1982, to appear.
5. R. GOMPF: Infinite families of Casson handles and topological disks *Topology* **23** (1984), 395–400.
6. R. GOMPF and S. SINGH: On Freedman's reimbedding theorems. *Four Manifold Theory*, Amer. Math. Soc. Summer Conference, University of New Hampshire, 1982; Amer. Math. Soc. Contemporary Math. **35** (1984).
7. J. MILNOR and D. HUSEMOLLER: *Symmetric Bilinear Forms*, Springer-Verlag, 1973.
8. R. A. NORMAN: Dehn's Lemma for certain 4-manifolds. *Invent. Math.* **7** (1969), 143–147.

*Department of Mathematics  
University of Texas  
Austin, TX 78712  
U.S.A.*